

# A numerical method to compute derivatives of functions of large complex matrices and its application to the overlap Dirac operator at finite chemical potential

Matthias Puhr<sup>a</sup>, Pavel Buividovich<sup>a</sup>

<sup>a</sup>*Institute of Theoretical Physics, Regensburg University, D-93053 Regensburg, Germany*

---

## Abstract

We present a method for the numerical calculation of derivatives of functions of general complex matrices. The method can be used in combination with any algorithm that evaluates or approximates the desired matrix function, in particular with implicit Krylov–Ritz-type approximations. An important use case for the method is the evaluation of the overlap Dirac operator in lattice Quantum Chromodynamics (QCD) at finite chemical potential, which requires the application of the sign function of a non-Hermitian matrix to some source vector. While the sign function of non-Hermitian matrices in practice cannot be efficiently approximated with source-independent polynomials or rational functions, sufficiently good approximating polynomials can still be constructed for each particular source vector. Our method allows for an efficient calculation of the derivatives of such implicit approximations with respect to the gauge field or other external parameters, which is necessary for the calculation of conserved lattice currents or the fermionic force in Hybrid Monte-Carlo or Langevin simulations. We also give an explicit deflation prescription for the case when one knows several eigenvalues and eigenvectors of the matrix being the argument of the differentiated function. We test the method for the two-sided Lanczos approximation of the finite-density overlap Dirac operator on realistic  $SU(3)$  gauge field configurations on lattices with sizes as large as  $14 \times 14^3$  and  $6 \times 18^3$ .

*Keywords:* chiral lattice fermions, finite density QCD, Krylov subspace methods, numerical differentiation

---

## 1. Introduction

Over the last decade matrix valued functions of matrices have become an essential tool in a variety of sub-fields of science and engineering [1]. An important application for matrix functions in the field of lattice QCD is the so-called overlap Dirac operator, which is a discretisation of the Dirac operator that respects the properly defined lattice chiral symmetry (Ginsparg-Wilson relations) and is free of doublers. Therefore the overlap Dirac operator is well suited for the non-perturbative study of strongly interacting chiral fermions. At finite

---

*Email addresses:* Matthias.Puhr@physik.uni-regensburg.de (Matthias Puhr), Pavel.Buividovich@physik.uni-regensburg.de (Pavel Buividovich)

chemical potential  $\mu$  the overlap Dirac operator is defined as [2]

$$D_{\text{ov}} := \frac{1}{a} (\mathbb{1} + \gamma_5 \text{sgn} [H(\mu)]), \quad (1)$$

where  $H(\mu) := \gamma_5 D_w(\mu)$ ,  $D_w(\mu)$  is the Wilson–Dirac operator at chemical potential  $\mu$ ,  $\text{sgn}$  is the matrix sign function and  $a$  stands for the lattice spacing. An explicit form of  $D_w(\mu)$  is given in Appendix A.

At finite chemical potential  $H$  is a non-Hermitian matrix with complex eigenvalues. Since the size of the linear space on which  $H$  is defined is typically very large ( $n \sim 10^4 \dots 10^7$ ), it is not feasible to evaluate the matrix sign function exactly. While at  $\mu = 0$  one can efficiently approximate the sign function of the Hermitian operator  $H$  by polynomials or rational functions [3–6], at nonzero  $\mu$  the operator  $H$  becomes non-Hermitian and such approximations typically become inefficient. However, having in mind that in practice the sign function  $\text{sgn} [H(\mu)]$  is applied to some source vector, one can still construct an efficient polynomial approximation for each particular source vector by using Krylov subspace methods, such as Krylov–Ritz-type approximations. One of the practical Krylov–Ritz-type approximations which are suitable for the finite-density overlap Dirac operator is the two-sided Lanczos (TSL) algorithm, developed in [7, 8]. The efficiency of the TSL approximation can be further improved by using a nested version of the algorithm [9].

Many practical tasks within lattice QCD simulations require the calculation of the derivatives of the lattice Dirac operator with respect to the gauge fields or some other external parameters. For example, conserved lattice vector currents and fermionic force terms in Hybrid Monte-Carlo simulations involve the derivatives of the Dirac operator with respect to Abelian or non-Abelian gauge fields. Also, electric charge susceptibilities which are used to quantify electric charge fluctuations in quark–gluon plasma involve derivatives of the Dirac operator with respect to the chemical potential.

While explicit expressions for the derivatives of source-independent approximations of matrix functions are well known and are routinely used in practical lattice QCD simulations, differentiating the implicit source-dependent approximation appears to be a more subtle problem. In principle the algorithms for taking numerical derivatives of scalar functions, like the finite difference method or algorithmic differentiation, can be generalised to matrix functions and to matrix function approximation algorithms. It is easy to combine an approximation with the finite difference method, but finite differences are very sensitive to round-off errors and it is often not possible to reach the desired precision in the derivative using this method. For algorithmic differentiation the situation is more complicated. Depending on the approximation method used it might not be immediately clear how to apply algorithmic differentiation. Even if algorithmic differentiation can be implemented for the approximation method this might lead to a numerically unstable algorithm. Such a behaviour was observed when the TSL approximation was used in conjunction with algorithmic differentiation [10].

In this paper, we propose and test a practical numerically stable method which makes it possible to compute derivatives of implicit approximations of matrix functions to high precision. The main motivation for this work is the need to take derivatives of the overlap Dirac operator in order to compute conserved currents on the lattice.

The structure of the paper is the following: in Section 2 we state some general theorems about matrix functions and their derivatives, which provide the basis for our numerical method. In Section 3 we discuss how the calculation of the derivatives of matrix functions can be made more efficient by deflating a number of small eigenvalues of the matrix which is the argument of the function being differentiated. The deflation is designed with the matrix sign function and the TSL approximation in mind. Nevertheless we want to emphasise that the method is very general and can be applied to other matrix functions and different matrix function approximation schemes. In Section 4 we demonstrate how the method can be used in practice. First we discuss the efficiency and convergence of the TSL approximation. After that, as a test case, we compute  $U(1)$  lattice vector currents, which involve the derivatives of the overlap Dirac operator with respect to background Abelian gauge fields, and demonstrate that they are conserved. Finally we summarise and discuss the advantages and disadvantages of our method in Section 5. Detailed calculations and derivations as well as a pseudo code implementation of the method can be found in the Appendices.

## 2. Matrix functions and numerical evaluation of their derivatives

For completeness we start this Section with a brief review of matrix functions. Let the function  $f : \mathbb{C} \rightarrow \mathbb{C}$  be defined on the spectrum of a matrix  $A \in \mathbb{C}^{n \times n}$ . There exist several equivalent ways to define the generalisation of  $f$  to a matrix function  $f : \mathbb{C}^{n \times n} \rightarrow \mathbb{C}^{n \times n}$  [1, 11]. For the purpose of this paper the most useful definition is via the Jordan canonical form. A well known Theorem states that any matrix  $A \in \mathbb{C}^{n \times n}$  can be written in the Jordan canonical form

$$X^{-1}AX = J = \text{diag}(J_1, J_2, \dots, J_k), \quad (2)$$

where every Jordan block  $J_i$  corresponds to an eigenvalue  $\lambda_i$  of  $A$  and has the form

$$J_i = J_i(\lambda_i) = \begin{pmatrix} \lambda_i & 1 & 0 & \cdots & 0 \\ 0 & \lambda_i & 1 & \ddots & \vdots \\ 0 & \ddots & \ddots & \ddots & 0 \\ \vdots & \ddots & \ddots & \lambda_i & 1 \\ 0 & \cdots & 0 & 0 & \lambda_i \end{pmatrix} \in \mathbb{C}^{m_i \times m_i}, \quad (3)$$

with  $m_1 + m_2 + \cdots + m_k = n$ . The Jordan matrix  $J$  is unique up to permutations of the blocks but the transformation matrix  $X$  is not. Using the Jordan canonical form the matrix function can be defined as [1, 11]

$$f(A) := Xf(J)X^{-1} = X \text{diag}(f(J_i))X^{-1}. \quad (4)$$

The function of the Jordan blocks is given by

$$f(J_i) := \begin{pmatrix} f(\lambda_i) & f'(\lambda_i) & \cdots & \frac{f^{(m_i-1)}(\lambda_i)}{(m_i-1)!} \\ 0 & f(\lambda_i) & \ddots & \vdots \\ \vdots & \ddots & \ddots & f'(\lambda_i) \\ 0 & \cdots & 0 & f(\lambda_i) \end{pmatrix} \in \mathbb{C}^{m_i \times m_i}, \quad (5)$$

Note that this definition requires the existence of the derivatives  $f^{(m_i-1)}(\lambda_i)$  for  $i = 1, \dots, k$ . If  $A$  is diagonalisable every Jordan block has size one and equation (5) reduces to the so-called spectral form

$$f(A) = X \operatorname{diag}(f(\lambda_1), f(\lambda_2), \dots, f(\lambda_n)) X^{-1}, \quad (6)$$

which does not depend on the derivatives of  $f$ . For instance, the matrix sign function  $\operatorname{sgn}[H(\mu)]$  in (1) is defined by  $\operatorname{sgn}(\lambda_i) = \operatorname{sgn}(\operatorname{Re} \lambda_i)$ .

Finding the Jordan normal form (or the spectral decomposition) of a matrix is a computationally expensive task and takes  $\mathcal{O}(n^3)$  operations. For large matrices it is therefore not feasible to compute the matrix function exactly. In practical calculations it is often sufficient to know the result  $|y\rangle = f(A)|x\rangle$  of the action of the matrix function on a vector and it is not necessary to explicitly compute the matrix  $f(A)$ . A variety of different methods have been developed to efficiently calculate an approximation of  $|y\rangle = f(A)|x\rangle$  (see chapter 13 of [1] for an overview). For non-Hermitian matrices  $A$  one typically constructs the approximation to  $|y\rangle$  using the Krylov subspaces spanned by the Krylov vectors  $A^k|x\rangle$  and  $(A^\dagger)^k|x\rangle$ ,  $k = 0, \dots, k_{max}$ . This implies that the approximation depends both on the matrix  $A$  itself and on the source vector  $|x\rangle$ . A practical example of such an approximation is the TSL algorithm of [7–9].

Let us now assume that the matrix  $A \equiv A(t)$  depends on some parameter  $t$ . In this work we are interested in the calculation of the derivative

$$\partial_t |y\rangle = (\partial_t f(A(t))) |x\rangle, \quad (7)$$

where  $\partial_t \equiv \frac{\partial}{\partial t}$  and the source vector  $|x\rangle$  is assumed to be independent of  $t$ . The practical method for calculating  $\partial_t |y\rangle$  which we propose here is based on the following Theorem [12]:

**Theorem 1.** *Let  $A(t) \in \mathbb{C}^{n \times n}$  be differentiable at  $t = 0$  and assume that the spectrum of  $A(t)$  is contained in an open subset  $\mathcal{D} \subset \mathbb{C}$  for all  $t$  in some neighbourhood of 0. Let  $f$  be  $2n - 1$  times continuously differentiable on  $\mathcal{D}$ . Then*

$$f(\mathcal{B}) \equiv \begin{pmatrix} f(A(0)) & \partial_t f(A(t))|_{t=0} \\ 0 & f(A(0)) \end{pmatrix}, \quad \mathcal{B}(A) := \begin{pmatrix} A(0) & \partial_t A(t)|_{t=0} \\ 0 & A(0) \end{pmatrix}$$

Theorem 1 relates the derivative of a matrix function  $\partial_t f(A)$  to the function of a block matrix  $f(\mathcal{B}(A))$ , and is in fact closely related to the formula (5). It is remarkable that one does not need to know the explicit form of  $\partial_t f$  to compute the derivative of  $f$ . This comes at the cost of evaluating the function  $f$  for the matrix  $\mathcal{B}$  that has twice the dimension of  $A$  and one needs to know the derivative  $\partial_t A$ . In practice  $\partial_t A$  is usually known analytically or can be computed to high precision. Moreover the block matrix  $\mathcal{B}$  is very sparse and one only needs to store  $A$  and  $\partial_t A$ . Thus Theorem 1 makes it possible to efficiently calculate the derivative of a matrix function.

Using Theorem 1 it is straightforward to compute the action of the derivative of a matrix function on a vector:

$$f(\mathcal{B}) \begin{pmatrix} 0 \\ |x\rangle \end{pmatrix} = \begin{pmatrix} \partial_t f(A)|x\rangle \\ f(A)|x\rangle \end{pmatrix} \quad (8)$$

Now one can use any matrix function approximation method to compute an approximation to the function  $f(\mathcal{B})$  in equation (8). To be specific we will use the TSL approximation for the rest of this paper, but any other approximation scheme can be used instead.

### 3. Spectral properties of the block matrix $\mathcal{B}$ and deflation of the derivatives of matrix functions

The convergence properties of the TSL approximation crucially depend on the spectrum of the matrix to which it is applied. In Appendix C we show that the spectrum of eigenvalues of  $\mathcal{B}$  is identical to the spectrum of  $A$ . Often the efficiency of the TSL approximation can be greatly improved by deflating a small number of eigenvalues. One might for example deflate the eigenvalues that are close to a pole of the function. For the matrix sign function it is advantageous to deflate the eigenvalues smallest in absolute value[7–9]. The standard deflation method relies on the diagonalisability of the matrix  $A$ . It is then straightforward to project out the eigenvectors corresponding to the deflated eigenvalues.

However the following Theorem states that, in general, the matrix  $\mathcal{B}$  is not diagonalisable:

**Theorem 2.** *Let  $A$  be a diagonalisable matrix. If  $\partial_t \lambda_i \neq 0$  for at least one eigenvalue  $\lambda_i$  of  $A$  then the matrix  $\mathcal{B}$  is not diagonalisable. If  $A$  has no degenerate eigenvalues and  $\partial_t \lambda_i \neq 0$  for all  $i \in \{1, \dots, n\}$  then every Jordan block in the Jordan normal form of  $\mathcal{B}$  is of size two, i.e.*

$$\mathcal{J} = \begin{pmatrix} J_1 & 0 & 0 & \dots & 0 \\ 0 & J_2 & \ddots & \ddots & \vdots \\ 0 & \ddots & \ddots & \ddots & 0 \\ \vdots & \ddots & \ddots & \ddots & 0 \\ 0 & \dots & 0 & 0 & J_n \end{pmatrix}, \quad J_i := \begin{pmatrix} \lambda_i & 1 \\ 0 & \lambda_i \end{pmatrix}.$$

The proof of this Theorem is somewhat technical and the main steps of the proof can be found in Appendix C. It follows directly from Theorem 2 that a matrix of the form  $\mathcal{B}$  does not possess a full basis of eigenvectors and it is therefore not immediately clear how to apply deflation to the numerical evaluation of equation (8).

In the following we develop a deflation method that is based on the Jordan normal form of  $\mathcal{B}$ . Since  $\mathcal{J}$  is the Jordan matrix of  $\mathcal{B}$  there exists an invertible matrix  $\mathcal{X}$  such that  $\mathcal{X}^{-1} \mathcal{B} \mathcal{X} = \mathcal{J}$ . Using Theorem 2 it is possible to derive an analytic expression for  $\mathcal{X}$  and  $\mathcal{X}^{-1}$  in terms of the eigenvalues and left and right eigenvectors of  $A$  and their derivatives. After some algebraic manipulations that are summarised in Appendix D we get

$$\mathcal{X}^{-1} = \begin{pmatrix} (\langle L_1 |, \langle \partial_t L_1 |) \\ \partial_t \lambda_1 (0, \langle L_1 |) \\ \vdots \\ (\langle L_n |, \langle \partial_t L_n |) \\ \partial_t \lambda_n (0, \langle L_n |) \end{pmatrix} \quad \text{and} \quad (9)$$

$$\mathcal{X} = \left( \begin{pmatrix} |R_1\rangle \\ 0 \end{pmatrix}, \frac{1}{\partial_t \lambda_1} \begin{pmatrix} |\partial_t R_1\rangle \\ |R_1\rangle \end{pmatrix}, \dots, \begin{pmatrix} |R_n\rangle \\ 0 \end{pmatrix}, \frac{1}{\partial_t \lambda_n} \begin{pmatrix} |\partial_t R_n\rangle \\ |R_n\rangle \end{pmatrix} \right), \quad (10)$$

where we used the eigenvalues  $\lambda_i$  and left (right) eigenvectors  $\langle L_i |$  ( $|R_i\rangle$ ) of  $A$ . The matrix  $\mathcal{X}^{-1}$  consists of  $2n$ -dimensional row vectors, i.e.

$$(\langle L_i |, \langle \partial_t L_i |) = (\langle L_i |_1, \dots, \langle L_i |_n, \langle \partial_t L_i |_1, \dots, \langle \partial_t L_i |_n). \quad (11)$$

Analogously  $\mathcal{X}$  is made up by  $2n$ -dimensional column vectors. With the help of the matrices  $\mathcal{X}$  and  $\mathcal{X}^{-1}$  we can define a generalised deflation. Let  $|x_i\rangle$  be the columns of  $\mathcal{X}$  and  $\langle \bar{x}_i |$  the rows of  $\mathcal{X}^{-1}$ , then  $\sum_{i=1}^{2n} |x_i\rangle \langle \bar{x}_i | = \mathbb{1}$ . We define the projectors  $\mathcal{P}_m = \sum_{i=1}^m |x_i\rangle \langle \bar{x}_i |$  and  $\bar{\mathcal{P}}_m := \mathbb{1} - \sum_{i=1}^m |x_i\rangle \langle \bar{x}_i |$ , such that for every vector  $|\psi\rangle$  we have

$$|\psi\rangle = \mathcal{P}_m |\psi\rangle + \bar{\mathcal{P}}_m |\psi\rangle \quad (12)$$

Now we have all the necessary ingredients to define a deflation algorithm for the matrix  $\mathcal{B}$ . Say we want to deflate the first  $2l$  eigenvalues of  $\mathcal{B}$  (corresponding to the first  $l$  eigenvalues  $\lambda_1, \dots, \lambda_l$  of  $A$ ). To calculate  $f(\mathcal{B})$  we split the evaluation of the function into two parts:

$$f(\mathcal{B}) |\psi\rangle = \mathcal{X} f(\mathcal{J}) \mathcal{X}^{-1} \mathcal{P}_{2l} |\psi\rangle + f(\mathcal{B}) \bar{\mathcal{P}}_{2l} |\psi\rangle \quad (13)$$

where we used equation (4) for the first term on the right side. To compute the function of the Jordan matrix we only need to consider the function for each Jordan block. Applying equation (5) to the  $j$ -th block of  $\mathcal{J}$  yields:

$$f(J_i) := \begin{pmatrix} f(\lambda_j) & \partial_t f(\lambda_j) \\ 0 & f(\lambda_j) \end{pmatrix} \quad (14)$$

Since the block structure of  $\mathcal{J}$  is preserved by the function and the  $|x_i\rangle$  and  $\langle \bar{x}_i |$  are biorthogonal one finds:

$$\begin{aligned} \mathcal{X} f(\mathcal{J}) \mathcal{X}^{-1} \mathcal{P}_{2l} |\psi\rangle = \\ \sum_{i=1}^l [f(\lambda_i) (|x_{2i-1}\rangle \langle \bar{x}_{2i-1} | \psi\rangle + |x_{2i}\rangle \langle \bar{x}_{2i} | \psi\rangle) + (\partial_t f(\lambda_i)) |x_{2j-1}\rangle \langle \bar{x}_{2i} | \psi\rangle] \end{aligned} \quad (15)$$

It is not necessary to compute the full transformation matrices  $\mathcal{X}$  and  $\mathcal{X}^{-1}$  since the rows and columns needed to evaluate equation (15) are known analytically in terms of the left and right eigenvectors of  $A$ . The latter can be efficiently computed using the Arnoldi algorithm (we have used the **ARPACK** implementation

[13]). In practical calculations one chooses  $2l \ll 2n$  and splits the calculation of  $f(\mathcal{B})$  in the following way

$$f(\mathcal{B})|\psi\rangle = \underbrace{f(\mathcal{B})\bar{\mathcal{P}}_{2l}|\psi\rangle}_{\text{TSL approximation}} + \underbrace{\sum_{i=1}^l [f(\lambda_i) (|x_{2i-1}\rangle \langle \bar{x}_{2i-1}| \psi\rangle + |x_{2i}\rangle \langle \bar{x}_{2i}| \psi\rangle) + (\partial_t f(\lambda_i)) |x_{2i-1}\rangle \langle \bar{x}_{2i}| \psi\rangle]}_{\text{exact}} \quad (16)$$

This looks very similar to the standard deflation formula for diagonalisable matrices. The difference is that now, because the Jordan blocks have size two, there is an additional “mixing term” proportional to  $\partial_t f(\lambda_i)$ . For the sign function equation (16) becomes even simpler. The sign function is piece-wise constant and for realistic gauge field configurations the eigenvalues of  $H$  do not cross the discontinuity line  $\text{Re}(z) = 0$  when an external parameter is varied. Therefore the derivative of the sign function  $\partial_t \text{sgn}(\lambda_i)$  is identically zero and the mixing term is absent in the deflation. A detailed explicit expression for the deflated derivative of the matrix sign function and the corresponding pseudocode can be found in Appendix E.

We note that in Hybrid Monte-Carlo simulations with dynamical overlap fermions it is possible that an eigenvalue  $\lambda_i$  of  $H$  crosses the discontinuity of the sign function at  $\text{Re} \lambda_i = 0$ , which corresponds to a change of the topological charge. The derivative of  $\text{sgn}(\lambda_i)$  in the last term in (16) then becomes singular. However, in practice such singularities in the fermionic force are typically avoided by modifying the Molecular Dynamics process in the vicinity of the singularity, for example by using the transmission-reflection step of [14, 15].

## 4. Numerical Tests for the overlap Dirac Operator

### 4.1. Numerical setup and tuning of the TSL algorithm

For the numerical tests we have used quenched  $SU(3)$  gauge configurations generated with the tadpole-improved Lüscher–Weisz action [16, 17]. The Wilson–Dirac operator with a background Abelian gauge field and finite quark chemical potential  $\mu$  is described in Appendix A. There we also give an analytic expression for the derivative  $\frac{\partial D_w(\mu)}{\partial \Theta_{x,\mu}}$  of the Wilson–Dirac operator with respect to the external lattice gauge field  $\Theta_{x,\mu}$ .

Before we discuss our results we give a detailed description of our numerical setup. The results in this Section were obtained using a nested version of the TSL algorithm [9]. We found that the main performance gains are already achieved with a single nesting step and that further nesting does not significantly improve the efficiency of the algorithm. Therefore for all our calculations we used only one level of nesting. In this case one has to choose two parameters for the Lanczos approximation, the sizes of the inner and outer Krylov subspace. For the TSL method it is not known how to compute a priori error estimates. In particular it is not possible to estimate which values for the Krylov subspace size parameters are necessary to reach a given precision in the calculation. An

a posteriori estimate for the numerical error  $\epsilon$  can be computed using the identity  $\text{sgn}(A)^2 = \mathbb{1}$ :

$$\epsilon_A = \frac{\|\text{sgn}(A)^2 |\psi\rangle - |\psi\rangle\|}{2 \|\psi\|}, \quad (17)$$

where  $\|\psi\| := \sqrt{\langle \psi | \psi \rangle}$  and the factor two was added because we have to apply the TSL approximation twice to compute the square of the sign function.

Similarly, in order to estimate the error  $\epsilon_B$  in the calculation of the derivative of the sign function we use the same formula as (17) where  $A$  is replaced by  $B$  and the vector  $|\psi\rangle$  is replaced by the sparse vector  $(0, |\psi\rangle)^T$ , i.e

$$\epsilon_B = \frac{\left\| \text{sgn}(B)^2 \begin{pmatrix} 0 \\ |\psi\rangle \end{pmatrix} - \begin{pmatrix} 0 \\ |\psi\rangle \end{pmatrix} \right\|}{2 \|\psi\|}. \quad (18)$$

We note that the square of the sign of the block matrix  $B$  is given by

$$\text{sgn}(B)^2 = \begin{pmatrix} \text{sgn}(A)^2 & \text{sgn}(A)(\partial_t \text{sgn}(A)) + (\partial_t \text{sgn}(A)) \text{sgn}(A) \\ 0 & \text{sgn}(A)^2 \end{pmatrix} \quad (19)$$

and the error estimate for the derivative as defined in equation (17) contains the anti-commutator  $\{\text{sgn}(A), \partial_t \text{sgn}(A)\}$  of the sign function and its derivative:

$$\epsilon_B = \sqrt{\left( \frac{\|\text{sgn}(A)^2 |\psi\rangle - |\psi\rangle\|}{2 \|\psi\|} \right)^2 + \left( \frac{\|\{\text{sgn}(A), \partial_t \text{sgn}(A)\} |\psi\rangle\|}{2 \|\psi\|} \right)^2}. \quad (20)$$

Note that the first summand in (20) is in general not equal to  $\epsilon_A^2$ , because the optimal polynomials approximating the sign functions of  $A$  and  $B$  are in general different. Since the square of the sign function is the identity the anti-commutator  $\{\text{sgn}(A), \partial_t \text{sgn}(A)\} = \partial_t(\text{sgn}(A)^2)$  should vanish and its deviation from zero can be used as an indicator of the precision with which the derivative  $\partial_t \text{sgn}(A)$  is calculated [10]. We found numerically that  $\epsilon_B$  gives a better estimate for the true error of the derivative and moreover it is easier to compute than the anti-commutator.

During production runs it is not feasible to check the error for every source vector  $|\psi\rangle$ . In general the optimal subspace sizes will depend on the matrix and on the source vector. If deflation techniques are used, however, the performance critical components of the source vector are projected out and treated exactly. Then it is reasonable to assume that for a given matrix the optimal parameter values will depend only weakly on the source vector. This suggests that it is possible to find a set of optimal parameters that will give the desired error for any vector. In order to find these optimal parameters we perform a ‘‘tuning run’’ for every gauge configuration:

- Select a target precision  $\epsilon_0$  (typically  $\epsilon_0 = 10^{-8}$ ).
- Select a trial vector  $|\phi\rangle$ . To compare different parameter sets the trial vector should be the same throughout the tuning run. Additionally it should be a good representation of the vectors that will be used in the production runs. Here we use  $|\phi\rangle = (1, \dots, 1)^\dagger$  to estimate the error  $\epsilon_A$  of  $\text{sgn}(A)$  and the sparse vector  $(0, |\phi\rangle)$  to estimate the error  $\epsilon_B$  of  $\text{sgn}(B)$ .

- Choose a set of trial parameters for the outer ( $k^O$ ) and inner ( $k^I$ ) Krylov subspace size  $p = \{(k_1^O, k_1^I), \dots, (k_m^O, k_m^I)\}$ . For every  $p_i \in p$  compute  $\epsilon_i := \epsilon(p_i)$  and the CPU time  $t_i := t(p_i)$  the TSL approximation took.
- Sort out all  $p_i$  for which  $\epsilon_i > \epsilon_0$
- From the remaining parameter sets  $p_j$  choose the one with the smallest  $t_j$
- Save the optimal parameters  $k_0^O$  and  $k_0^I$  for use in the production runs

Of course there is no guaranty that for some vector other than the trial vector  $|\phi\rangle$  the parameters  $k_0^O$  and  $k_0^I$  found in the tuning run will give an error smaller than  $\epsilon_0$ . One way to validate the results from the tuning run is to perform a cross check:

- Use  $k_0^O$  and  $k_0^I$  to compute the error for  $l$  random vectors (in practice,  $l = 20 \dots 30$ )
- Check if the maximal error for all random vectors is smaller than  $\epsilon_0$ .

If the maximal error is found to be too large one can restart the tuning run with a different trial vector to get better estimates for the optimal parameters. We found that in most cases the error for the random vectors has the same order of magnitude as the error for the trial vector. As a rule of thumb if one wants to achieve a precision  $\epsilon_0$  one should use the target precision  $10^{-1}\epsilon_0$  for the trial run.

The TSL algorithm implicitly generates a polynomial approximation of the sign function. The highest order of the approximation polynomial is given by the size of the outer Krylov subspace. Another way to test the validity of the optimal parameter estimate obtained in the trial run is to compare the results of the TSL approximation to some other method. To this end we have set  $\mu = 0$  and compared the relative error of the TSL approximation with the error of the minmax polynomial approximation [4], which works well when  $H$  is a Hermitian operator.

In Figure 1 we compare the error of the TSL approximation for a given outer Krylov subspace size with the minmax polynomial result. The error estimate (17) for  $\text{sgn}(H)$  is computed for 10 random vectors on 20 different gauge configurations of size  $8 \times 8^3$  (corresponding to a matrix of dimension  $n = 49152$ ) with  $\beta = 8.1$ . For these parameters the spectrum of  $H$  has only a small gap around the line  $\text{Re}(z) = 0$ , which makes it more difficult to approximate the matrix sign function with a polynomial of low order. To improve both the TSL and the minmax approximation we deflated the 30 eigenvalues with the smallest absolute value in our calculations.

The mean error is computed by averaging over random vectors and gauge configurations and we plot the mean error as a function of the maximal power of  $H$  in the approximating polynomial (for the nested TSL algorithm, this is the size of the outer Krylov subspace). The results are shown in Figure 1. We find that at fixed polynomial degree the error for the TSL method is smaller than the error of the minmax polynomial by almost an order of magnitude. This is to be expected, since the minmax polynomial tries to minimise the maximal error over all vectors, while the TSL method constructs a different and optimised polynomial for every source vectors. For large matrices the main

computational cost comes from matrix vector products and the overhead of different algorithms for finding the optimal coefficients of the approximating polynomial becomes negligible. The minmax polynomial method generates a polynomial in  $H^2$ , while the TSL method constructs the Krylov subspaces for both  $H$  and  $H^\dagger$ . Moreover, since storing all the Krylov vectors requires very large RAM memory and is hardly feasible in practice, we have used a two-pass version of the TSL method. The first pass is used to find the coefficients of the optimal approximating polynomial, and the second pass to calculate this polynomial with known coefficients. Because of the twice larger number of vectors used to construct the Krylov subspace and the need to calculate these vectors twice, for a given order of the approximating polynomial the minmax approach is roughly four times faster. The CPU time of the two algorithms is compared in Figure 1. Our numerical test for  $8 \times 8^3$  configurations shows that

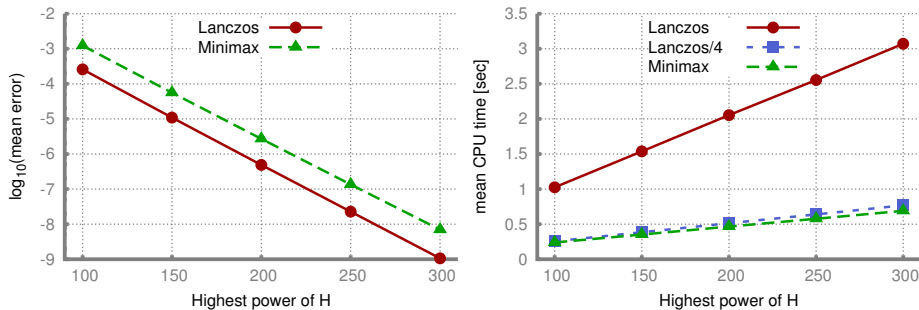


Figure 1: Comparison of the TSL approximation with the minmax polynomial method. On the left we show the mean error of both methods as a function of the highest power of the polynomial. The plot on the right shows the mean time required for the calculation of  $\text{sgn}(H)|x$  on an Intel<sup>®</sup> Core<sup>™</sup> i5-3470 CPU, with multi-core OpenBLAS [18] used for basic linear algebra. As expected the TSL is slower than the minmax polynomial approach by a factor of four.

the error of the TSL method does not strongly depend on the source vector and that it is almost an order of magnitude smaller than one would expect from a naive comparison with other approximation methods. For our production runs we therefore use a single tuning run to find an estimate for the optimal parameters. The parameter set found in this way is then used for all further calculations.

#### 4.2. TSL approximation for the derivatives of the sign function

After tuning the TSL approximation for the sign function  $\text{sgn}(H)$ , we are now ready to apply it to the block matrix  $\mathcal{B}(H)$ . Motivated by the practical calculations of conserved vector currents on the lattice, we assume that the parameter  $t$  is the Abelian lattice gauge field  $\Theta_{x,\mu}$  on the link which goes in the direction  $\mu$  from the lattice site  $x$ .

In Figure 2 we show typical results for the error of  $\text{sgn}(H)$  and  $\text{sgn}(\mathcal{B}(H))$  at  $\mu = 0$  as a function of the outer Krylov subspace size for gauge configurations ranging in size from  $4 \times 4^3$  ( $n = 3072$ ) to  $14 \times 14^3$  ( $n = 460992$ ). The benefit of the deflation is clearly visible. In the computation of the derivatives the deflation process has an additional positive side effect. To evaluate derivatives we have to take a sparse input vector. Moreover the derivative matrix in lattice

QCD is very sparse, since the change of a single link influences only two lattice sides. Therefore the vectors generated by the TSL algorithm have a sparse upper part and the Krylov subspace does not efficiently approximate the full space. By projecting out the vectors corresponding to the eigenvalues near zero the sparse pattern of the source vector is destroyed and the Krylov subspace has a more general form which positively influences the convergence rate of the method. Figure 2 shows that the method scales very well with the lattice volume. For the configuration with  $V = 6 \times 18^3$  and  $\beta = 8.45$  the temperature is already above the deconfinement transition temperature for the Lüscher–Weisz action [19], hence there is already a large gap in the spectrum of  $H$  and the deflation has only a minor effect on the efficiency of the TSL method.

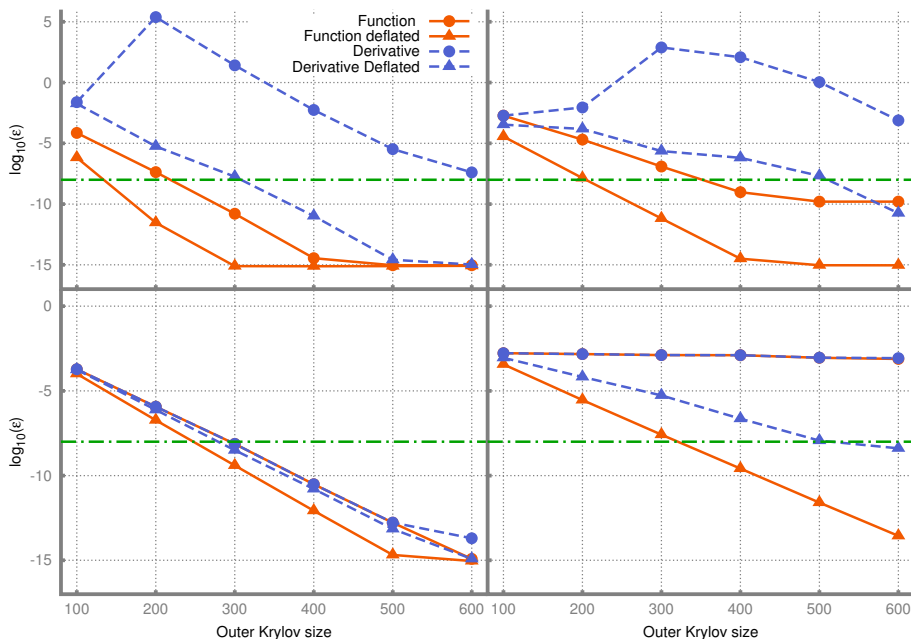


Figure 2: Matrix size dependence of the optimal outer Krylov subspace size for zero chemical potential. The green, dash-dotted line marks the desirable error of  $10^{-8}$ . (Un-)deflated results are marked by (circular) triangular symbols. The data points are connected with lines to guide the eye. A solid line stands for the sign function results while a broken line indicates the results for the derivative. Clockwise from top left the results are shown for  $4 \times 4^3$ ,  $6 \times 6^3$ ,  $14 \times 14^3$  and  $6 \times 18^3$  lattices. For  $4 \times 4^3$ ,  $6 \times 6^3$ ,  $14 \times 14^3$  lattices we have used  $\beta = 8.1$  ( $a = 0.125$  fm) and for  $6 \times 18^3$  lattice we have used  $\beta = 8.45$  ( $a = 0.095$  fm). The inner Krylov subspace size is set to 100 in all plots. For the deflation of the sign function we use the 40 eigenvalues with the smallest magnitude. To deflate the derivative, we have used two eigenvalues for  $4 \times 4^3$ ,  $6 \times 6^3$  and  $6 \times 18^3$  lattices and six eigenvalues for  $14 \times 14^3$ .

An interesting question is how the optimal Krylov subspace size for a given error depends on the chemical potential. As the chemical potential is increased the operator  $H$  deviates more and more from a Hermitian matrix and one expects that a larger Krylov subspace size is necessary to achieve a given accuracy. We indeed observe this behaviour and Figure 3 shows the results for the error at different values of  $\mu$ . From the plots we can estimate that at  $\mu = 0$  an outer Krylov subspace size of 500 is sufficient to obtain an error of  $10^{-8}$  for the deflated derivative for the  $V = 14 \times 14^3$  configuration. For  $\mu = 0.05$  one has to

use a subspace size of roughly 600 for the same error. At  $\mu = 0.3$  it seems that the error can be achieved with a subspace size of around 650. Going from zero chemical potential to a finite value of  $\mu = 0.05$  makes it necessary to increase the Krylov subspace size by about 20%. Once the chemical potential is switched on, however, the increase in the Krylov subspace size is not that dramatic. Between  $\mu = 0.05$  and the rather large value  $\mu = 0.30$  the increase in the Krylov subspace size is roughly 10%. For the  $V = 6 \times 18^3$  configuration switching on

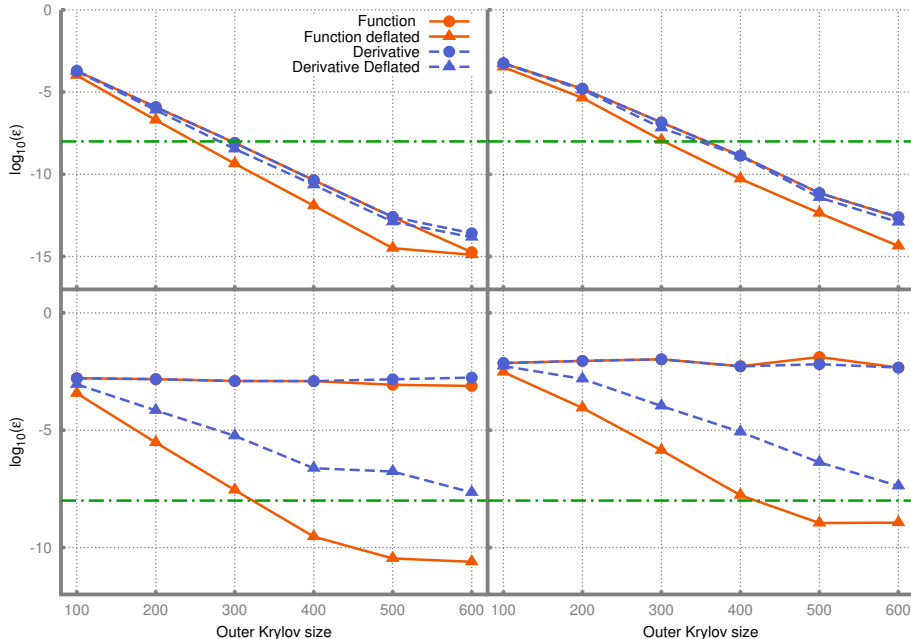


Figure 3: Chemical potential dependence of the error as a function of the outer Krylov subspace size. Top:  $V = 6 \times 18^3$  and  $\mu = 0.04$  on the left and  $\mu = 0.23$  on the right. Bottom:  $V = 14 \times 14^3$  and  $\mu = 0.05$  on the left and  $\mu = 0.3$  on the right. All other parameters are the same as for Figure 2.

a small chemical potential only has a negligible effect on the error for a given Krylov subspace size. If  $\mu = 0.23$  one has to take a Krylov subspace size of approximately 350 to get an error of  $10^{-8}$ . Compared to the Krylov subspace size of 280 for  $\mu = 0$  this is an increase of about 25%.

#### 4.3. Divergence of $U(1)$ vector current

As a further practice-oriented test of our method, we now consider the divergence of the  $U(1)$  vector current

$$\delta j_x = \sum_{\mu} (j_{x,\mu} - j_{x-\mu,\mu}) \quad (21)$$

at a randomly chosen lattice site  $x$  for a fixed gauge field configuration which was randomly selected from an ensemble of equilibrium gauge field configurations. For a fixed gauge field configuration, the current  $j_{x,\mu}$  flowing in the direction  $\mu$  from the lattice site  $x$  is given by

$$j_{x,\mu} = \text{tr} \left( D_{\text{ov}}^{-1} \frac{\partial D_{\text{ov}}}{\partial \Theta_{x,\mu}} \right). \quad (22)$$

Invariance of the Dirac operator under the gauge transformations  $\Theta_{x,\mu} \rightarrow \Theta_{x,\mu} + \phi_x - \phi_{x+\mu}$  demands that the divergence of the vector current at a given lattice site vanishes.

For small lattice sizes the trace in (22) can be calculated exactly, but for larger volumes this is no longer feasible. We use stochastic estimators with  $Z_2$ -noise [20] to compute an approximation of the trace for all currents in (21). The error bars on our results are given by the standard estimate for the error of the sample mean.

As a further check we additionally compute the “total current” at a lattice site, which is just the sum over incoming and outgoing currents (replacing the minus sign in (21) with a plus). This quantity has no physical meaning and can take any value. If the total current is not zero an exact cancellation is necessary to achieve a vanishing divergence. Finding numerically that the divergence vanishes even when the total current does not can be seen as an additional cross check. Figure 4 shows the results for the divergence and the total current at finite  $\mu$  for two configurations of different size. For both configurations we find that the total current has a finite value but the divergence vanishes as the number of stochastic estimators is increased.

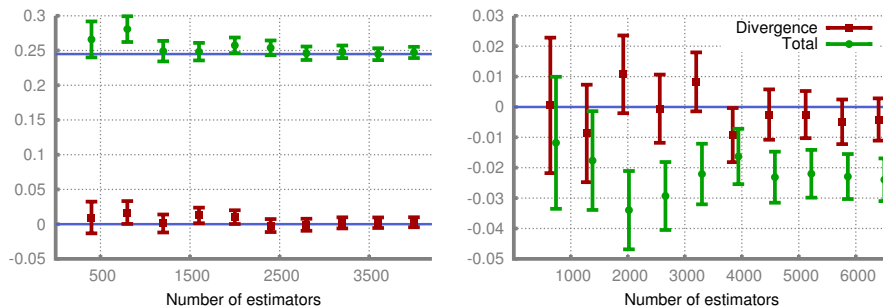


Figure 4: Results for divergence (red squares) of the vector current and the total current (green circles) at a lattice site for configurations with  $\beta = 8.1$  and  $\mu = 0.3$ , plotted as functions of the number of stochastic estimators. On the left  $V = 3 \times 4^3$ . For this small configuration the exact values can be computed and are indicated by solid blue lines. On the right  $V = 6 \times 6^3$ . Here it is not feasible to compute the exact values. The results for the total current are shifted by 100 estimators to the right for better visibility and the blue line marks zero.

Results for larger configurations are shown in Figure 5. Computing a large number of stochastic estimators is very expensive even for relatively small lattice sizes. For the larger lattices we therefore studied the current conservation only for the case  $\mu = 0.0$ . We found that the divergence of the current as well as the total current is very small for both configurations. To see a clear separation between the divergence and the total current one would have to significantly increase the number of stochastic estimators. The value of the divergence is in both cases consistent with zero and we emphasise that the error bars clearly show the expected inverse square root dependence on the number of estimators.

## 5. Discussion and conclusions

In this work we have proposed and tested an efficient numerical method to compute derivatives of matrix functions of general complex matrices. In

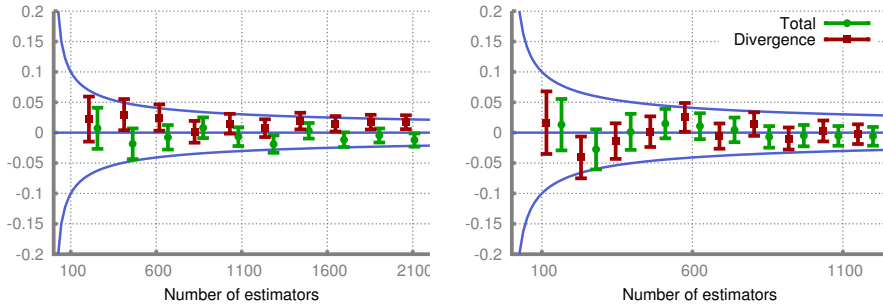


Figure 5: Results for divergence and the sum of the vector current at a lattice site for large lattices, plotted as functions of the number  $n_e$  of stochastic estimators. Left  $V = 6 \times 18^3$  with  $\beta = 8.45$ , right  $V = 14 \times 14^3$  with  $\beta = 8.1$ . The chemical potential is  $\mu = 0.0$  for both plots. The results for the total current are shifted by 50 estimators to the right for better visibility. The straight blue line marks zero and the curved blue lines depicting  $\pm 1/\sqrt{n_e}$  are drawn to visualise the error dependence on the number of estimators.

particular we have shown that our method in combination with the TSL approximation can be used to compute derivatives of the matrix sign function with high precision. When one computes an approximation of a matrix function it is often possible to improve the efficiency of the algorithm by deflating a relatively small number of eigenvalues and treating them exactly. For this reason we have also presented a generalised deflation method that does not depend on the diagonalisability of the matrix.

In practical calculations it is important to know (an estimate for) the error of an algorithm. We give a heuristic for tuning the parameters of our method to a given error. To check how reliable the error estimate is we computed the error for a variety of random source vectors on a number of medium sized ( $8 \times 8^3$ ) gauge configurations. As a cross check we compared the errors of the TSL approximation with the errors obtained by a minmax polynomial approximation. We found that our heuristic works very well and gives a good error estimate. The error of the TSL method is consistently lower than the error of the minmax polynomial by almost an order of magnitude. The TSL method constructs two Krylov subspaces and we have to use a double-pass version of the algorithm because of memory limitations, which makes the TSL method about a factor of four slower than the minmax polynomial for a given order of the interpolating polynomial. We note that our findings suggest that a Lanczos type algorithm that is optimised for Hermitian matrices could outperform the minmax polynomial approximation. The Lanczos method for Hermitian matrices constructs only one Krylov subspace size, which reduces the computational effort and the memory requirements by a factor two. Therefore a single-pass version of the Lanczos algorithm could be feasible even for relatively large Hermitian matrices. At a given precision, such an algorithm would be considerably faster than the minmax approximation.

We have tested our method for the derivatives of the finite-density overlap Dirac operator on different gauge configurations and for different values of the chemical potential  $\mu$ . The higher the value of  $\mu$  the more the operator  $H$  differs from a Hermitian matrix. We find that our method performs very well even for large values of  $\mu$  up to 470 MeV in physical units and that the Krylov subspace

size necessary to achieve a given error does not strongly depend on  $\mu$ . For all configurations we compared the deflated and the undeflated version of the algorithm. With our choice of parameters in the confining phase the operator  $H$  in general only has a rather small gap in the spectrum around the discontinuity line  $\text{Re}(z) = 0$  and deflation greatly improves the performance of the method. On the other hand we find numerically that in the deconfinement phase the gap in the spectrum of  $H$  is larger and there are no eigenvalues with real part close to zero. In this case the deflation has only a minor effect.

In the deflated version of our method a large fraction of the overall CPU time is spent for the inversion of the matrices  $A_{\lambda_i} = \lambda_i - A$  in equation (E.4). All the inversions act on the same source vector and if it is possible to use a multi-shift algorithm for the inversions the performance of the method could be significantly improved. We tried to use the BiCGSTAB algorithm to compute  $A_{\lambda_i}^{-1}$ , since multi-shift versions of this algorithm exist. It turned out, however, that this approach is numerically unstable and in the end we computed the inverse by applying the CG algorithm to the matrix  $A_{\lambda_i} A_{\lambda_i}^\dagger$ . Thus finding a suitable multi-shift inverter is one of the possible ways to speed up our algorithm.

Equivalents of Theorem 1 exist also for higher order derivatives of matrix functions [21] and in principle it is straightforward to generalise our method for higher derivatives. To compute the  $k$ -th derivative of a function of a  $n$ -dimensional matrix one has to construct an upper-triangular block matrix of dimension  $(k + 1)n$ . In particular, second-order derivatives are required for the calculation of current-current and charge-charge correlators, from which one can extract electric conductivity and charge diffusion rate. However, in the case of higher derivative the expressions for the deflated derivatives become extremely complicated. It seems thus that the only practical way to calculate higher derivatives is to avoid deflation, which necessarily involves restriction to small lattice sizes or to high temperatures.

An important application of our method and the main motivation for this work is the computation of conserved currents for the finite-density overlap Dirac operator in lattice QCD. Conserved currents and current-current correlators are important observables for the study of anomalous transport effects such as the Chiral Magnetic [22] or the Chiral Separation [23, 24] effects. These dissipationless parity-odd transport effects, which originate from the chiral anomaly, have recently become the focus of intensive studies in both high-energy and solid-state physics. While the anomalous transport for free chiral fermions is well understood, there are still many interesting open questions for strongly interacting fermions. With our method it is possible to efficiently study anomalous transport for strongly interacting chiral fermions on the lattice at finite quark chemical potential.

## 6. Acknowledgements

We thank Andreas Frommer for pointing us to Theorem 1, and Jacques Bloch and Simon Heybrock for useful discussions of the Lanczos approximation. This work was supported by the S. Kowalewskaja award from the Alexander von Humboldt Foundation.

## Appendix A. The Wilson–Dirac operator and its derivative

The Wilson–Dirac operator  $D_w(\mu)$  for a single quark flavour at finite quark chemical potential  $\mu$  and in the presence of a background  $U(1)$  gauge field can be written as

$$D_w(\mu) = \mathbb{1} - \kappa \sum_{i=1}^3 (G_i^+ + G_i^-) - \kappa (e^\mu G_4^+ + e^{-\mu} G_4^-), \quad (\text{A.1})$$

with

$$(G_\nu^\pm)_{x,y} := (1 \pm \gamma_\nu) U_{\pm\nu}(x) e^{i\Theta_{\pm\nu}(x)} \delta_{x\pm\hat{\nu},y}. \quad (\text{A.2})$$

The  $U_{\pm\nu}(x) \in SU(3)$  are (dynamical) lattice gauge fields and the factors  $e^{i\Theta_{\pm\nu}(x)} \in U(1)$  describe the (background) lattice gauge fields corresponding to the external Abelian gauge field  $\Theta_\nu(x)$ . We set the lattice spacing to one and define the hopping parameter  $\kappa := 1/(2m_W + 8)$ , where  $m_W \in (0, 2)$  is the Wilson mass term. The matrices  $\gamma_\nu$  are the Euclidean Dirac matrices.

Computing the derivative of the Wilson–Dirac operator with respect to the Abelian gauge field is straightforward and the result reads as

$$\left( \frac{\partial D_w}{\partial \Theta_\nu(z)} \right)_{x,y} = -i\kappa \left( (G_\nu^+)_{x,y} \delta_{x,z} - (G_\nu^-)_{x,y} \delta_{x-\hat{\nu},z} \right). \quad (\text{A.3})$$

## Appendix B. Derivatives of eigenvectors and eigenvalues

In this Appendix we formally define the notion of the derivative of eigenvectors and summarise some useful results.

Let  $A(t)$  be a diagonalisable matrix which depends on a parameter  $t$  and has eigenvalues  $\lambda_i$  and (left) eigenvectors  $(\langle L_i | | R_i \rangle)$ . For brevity we assume that  $A$  has no degenerate eigenvalues, i.e.  $\lambda_i \neq \lambda_j$  if  $i \neq j$ . For the Wilson–Dirac operator on real lattice QCD configurations, this is usually the case, since configurations with degenerate eigenvalues form a set of measure zero in the space of all gauge field configurations.

If  $|R_j\rangle$  is an eigenvector of  $A$  so is  $\alpha |R_j\rangle$  for any  $\alpha \in \mathbb{C} \setminus \{0\}$ . The direction of an eigenvector is fixed, but its norm and phase are not. In practice a common choice is to fix the eigenvectors by requiring that the left and right eigenvectors are bi-orthonormal:

$$\langle L_i | R_j \rangle = \delta_{ij} \quad (\text{B.1})$$

In general  $\alpha$  can be any non-vanishing differentiable function  $\alpha(t)$ . The freedom in choosing  $\alpha$  leads to a freedom in the norm and the direction of the derivative of the eigenvector, since

$$\partial_t (\alpha |R_j\rangle) = \alpha |\partial_t R_j\rangle + (\partial_t \alpha) |R_j\rangle \quad (\text{B.2})$$

This means the derivative of an eigenvector is fixed only up to a multiplication with a scalar and the addition of any vector from  $\text{span}(|R_j\rangle)$ . Therefore it is necessary to specify which one of all this possible derivatives is used in a certain calculation. Requiring the normalisation (B.1) only leads to the restriction  $\text{Re}(\langle L_j | \partial_t R_j \rangle) = 0$  and does not fully fix the derivatives of the eigenvectors. Throughout this paper we will therefore employ the additional constraint

$$\langle L_j | \partial_t R_j \rangle = 0 \quad (\text{B.3})$$

so that the derivative of an eigenvector is well defined. It is always possible to choose the eigenvectors such that (B.3) is fulfilled. Note that condition (B.1) does not fix the norm of the vectors  $|R_j\rangle$  and  $\langle L_j|$ . Suppose we found vectors that obey (B.1). Then  $\langle L_j|\partial_t R_j\rangle = \xi$ , where  $\xi$  is either zero or purely imaginary. If we now define  $|\overline{R}_j\rangle := e^{-\xi t}|R_j\rangle$  and  $\langle\overline{L}_j| := \langle L_j|e^{\xi t}$  we find that  $\langle\overline{L}_j|\overline{R}_j\rangle = 1$  and  $\langle\overline{L}_j|\partial_t\overline{R}_j\rangle = 0$ .

Using the definitions above we will now derive some useful relations. We start with the eigenvalue equation

$$A|R_j\rangle = \lambda_j|R_j\rangle. \quad (\text{B.4})$$

Taking the derivative on both sides yields

$$(\partial_t A)|R_j\rangle + A|\partial_t R_j\rangle = (\partial_t \lambda_j)|R_j\rangle + \lambda_j|\partial_t R_j\rangle. \quad (\text{B.5})$$

Multiplying from the left by  $\langle L_j|$  gives the following relation for the derivative of the eigenvalue:

$$\langle L_j|(\partial_t A)|R_j\rangle = \partial_t \lambda_j \quad (\text{B.6})$$

To derive a similar result for the derivative of the eigenvectors multiply (B.5) from the left by  $\langle L_i|$  for some  $i \neq j$ . With the normalisation (B.1) this gives

$$\langle L_i|(\partial_t A)|R_j\rangle + \lambda_i\langle L_i|\partial_t R_j\rangle = \lambda_j\langle L_i|\partial_t R_j\rangle. \quad (\text{B.7})$$

Therefore the following equation holds for  $i \neq j$ :

$$\langle L_i|\partial_t R_j\rangle = \frac{\langle L_i|(\partial_t A)|R_j\rangle}{\lambda_j - \lambda_i} \quad (\text{B.8})$$

Multiplying this equation by  $|R_i\rangle$  from the left and summing over  $i \neq j$  yields

$$|\partial_t R_j\rangle = \sum_{i \neq j} \frac{|R_i\rangle \langle L_i|(\partial_t A)|R_j\rangle}{\lambda_j - \lambda_i}, \quad (\text{B.9})$$

where we used (B.3) and the identity  $\sum_{i=1}^n |R_i\rangle \langle L_i| = \mathbb{1}$  to make the replacement

$\sum_{i \neq j} |R_i\rangle \langle L_i|\partial_t R_j\rangle = \sum_{i=1}^n |R_i\rangle \langle L_i|\partial_t R_j\rangle = |\partial_t R_j\rangle$ . Similarly we obtain for the derivative of the left eigenvectors

$$\langle\partial_t L_j| = \sum_{i \neq j} \frac{\langle L_j|(\partial_t A)|R_i\rangle \langle L_i|}{\lambda_j - \lambda_i}. \quad (\text{B.10})$$

### Appendix C. Properties of the block matrix $\mathcal{B}$

The convergence properties of matrix function approximation methods in general depend on the spectrum of the matrix. It is therefore important to know the spectrum of  $\mathcal{B}$ . Let  $\mathcal{B}$  be defined as in Theorem 1 and let  $\lambda_i$ ,  $i = 1, \dots, n$  be the eigenvalues of  $A$ . Since  $\mathcal{B}$  is an upper block matrix  $\det(\mathcal{B}) = \det(A)\det(A) = \det(A)^2$ . From this it immediately follows that the eigenvalues of  $\mathcal{B}$  are degenerate and identical to the  $\lambda_i$ .

A matrix is diagonalisable if and only if its minimal polynomial is a product of *distinct* linear factors. We will now discuss the outline of a proof of Theorem 2, which states that in general the matrix  $\mathcal{B}$  is not diagonalisable. In the following we assume that  $A$  has no degenerate eigenvalues to simplify the argumentation. The generalisation to the case of degenerate eigenvalues is possible but a bit more involved. For every eigenvalue  $\lambda_i$  of  $A$  we define the two vectors

$$|v_{i,1}\rangle := \begin{pmatrix} |R_i\rangle \\ 0 \end{pmatrix} \quad \text{and} \quad |v_{i,2}\rangle := \begin{pmatrix} |\partial_t R_i\rangle \\ |R_i\rangle \end{pmatrix}. \quad (\text{C.1})$$

It is easy to convince oneself that these vectors are linearly independent and that  $|v_{i,1}\rangle$  is an eigenvector of  $\mathcal{B}$  to the eigenvalue  $\lambda_i$ . For  $|v_{i,2}\rangle$  we have

$$\begin{aligned} \mathcal{B}|v_{i,2}\rangle &= \begin{pmatrix} A|\partial_t R_i\rangle + (\partial_t A)|R_i\rangle \\ A|R_i\rangle \end{pmatrix} = \begin{pmatrix} \partial_t(A|R_i\rangle) \\ A|R_i\rangle \end{pmatrix} \\ &= \begin{pmatrix} \lambda_i|\partial_t R_i\rangle + (\partial_t \lambda_i)|R_i\rangle \\ \lambda_i|R_i\rangle \end{pmatrix} = \lambda_i|v_{i,2}\rangle + (\partial_t \lambda_i)|v_{i,1}\rangle. \end{aligned} \quad (\text{C.2})$$

The vector  $|v_{i,2}\rangle$  is an eigenvector of  $\mathcal{B}$  only if  $\partial_t \lambda_i$  vanishes. If  $\partial_t \lambda_i \neq 0$  we find

$$(\mathcal{B} - \lambda_i \mathbb{1})^2 |v_{i,2}\rangle = (\partial_t \lambda_i)(\mathcal{B} - \lambda_i \mathbb{1}) |v_{i,1}\rangle = 0 \quad (\text{C.3})$$

and therefore  $|v_{i,2}\rangle$  is a generalised eigenvector of rank two corresponding to the eigenvalue  $\lambda_i$ . From this and the fact that the algebraic multiplicity of the eigenvalue  $\lambda_i$  of  $\mathcal{B}$  is two it immediately follows that the multiplicity of  $\lambda_i$  in the minimal polynomial of  $\mathcal{B}$  is also two. This proves the first part of Theorem 2.

To see that the second part of Theorem 2 is true, note that for every eigenvalue of  $A$  we have at least one Jordan block. Moreover the size of the largest Jordan block belonging to an eigenvalue  $\lambda_i$  is the multiplicity of the eigenvalue in the minimal polynomial. Therefore if the eigenvalues are all pairwise distinct there are at least  $n$  Jordan blocks of size 2 and since the dimension of  $\mathcal{B}$  is  $2n$  this proves the Theorem.

#### Appendix D. Derivation of the Jordan Decomposition

The aim of this appendix is to derive the analytic form of the Jordan decomposition of  $\mathcal{B}$  in terms of the eigenvectors and eigenvalues of  $A$ . In practice one never encounters a matrix  $A$  with degenerate eigenvalues. Moreover if one or more of the derivatives of the eigenvalues of  $A$  vanishes the Jordan matrix of  $\mathcal{B}$  only becomes simpler. Therefore in this paper we assume that every Jordan block of  $\mathcal{B}$  is of size two. The generalisation to the case where some of the Jordan blocks have size one is straightforward.

If  $\mathcal{J}$  is the Jordan normal form of the matrix  $\mathcal{B}$  there exists an invertible matrix  $\mathcal{X}$  such that  $\mathcal{X}^{-1}\mathcal{B}\mathcal{X} = \mathcal{J}$ , i. e.

$$\mathcal{B}\mathcal{X} = \mathcal{X}\mathcal{J} \quad (\text{D.1})$$

The exact form of the Jordan matrix  $\mathcal{J}$  follows from Theorem 2 and can be exploited to compute the transformation matrix  $\mathcal{X}$ . In bra-ket notation the

transformation matrix reads as  $\mathcal{X} := (|x_1\rangle, \dots, |x_{2n}\rangle)$ . Evaluating the right hand side of equation (D.1) yields

$$\begin{pmatrix} x_{1,1} & \dots & x_{1,2n} \\ \vdots & & \vdots \\ x_{2n,1} & \dots & x_{2n,2n} \end{pmatrix} \begin{pmatrix} \lambda_1 & 1 & 0 & \dots & 0 \\ 0 & \lambda_1 & \ddots & \ddots & \vdots \\ \vdots & \ddots & \ddots & \ddots & 0 \\ \vdots & & \ddots & \lambda_n & 1 \\ 0 & \dots & \dots & 0 & \lambda_n \end{pmatrix} = \quad (\text{D.2})$$

$$\begin{pmatrix} \lambda_1 x_{1,1} & x_{1,1} + \lambda_1 x_{1,2} & \dots & \lambda_n x_{1,(2n-1)} & x_{1,(2n-1)} + \lambda_n x_{1,2n} \\ \vdots & \vdots & & \vdots & \vdots \\ \lambda_1 x_{2n,1} & x_{2n,1} + \lambda_1 x_{2n,2} & \dots & \lambda_n x_{2n,(2n-1)} & x_{2n,(2n-1)} + \lambda_n x_{2n,2n} \end{pmatrix}$$

Combining equations (D.1) and (D.2) leads to  $n$  coupled equations

$$\mathcal{B} |x_{(2j-1)}\rangle = \lambda_j |x_{(2j-1)}\rangle \quad (\text{D.3})$$

$$\mathcal{B} |x_{2j}\rangle = |x_{(2j-1)}\rangle + \lambda_j |x_{2j}\rangle, \quad (\text{D.4})$$

where  $j \in \{1, n\}$ . Equation (D.3) is just the eigenvalue equation for the matrix  $\mathcal{B}$  and is easy to solve. Assume that  $|R_j\rangle$  is an eigenvector of  $A$  to the eigenvalue  $\lambda_j$ , then it is straightforward to show that  $(|R_j\rangle, 0)^T$  is an eigenvector of  $\mathcal{B}$  to the same eigenvalue.

Using the solution of equation (D.3) and defining  $|x_{2j}\rangle := (|x_{j,1}\rangle, |x_{j,2}\rangle)^T$  equation (D.4) can be written as

$$\begin{pmatrix} A & \partial_t A \\ 0 & A \end{pmatrix} \begin{pmatrix} |x_{j,1}\rangle \\ |x_{j,2}\rangle \end{pmatrix} = \begin{pmatrix} |R_j\rangle \\ 0 \end{pmatrix} + \lambda_j \begin{pmatrix} |x_{j,1}\rangle \\ |x_{j,2}\rangle \end{pmatrix} \quad (\text{D.5})$$

which simplifies to

$$(A - \lambda_j) |x_{j,1}\rangle + (\partial_t A) |x_{j,2}\rangle = |R_j\rangle \quad \text{I} \quad (\text{D.6})$$

$$(A - \lambda_j) |x_{j,2}\rangle = 0 \quad \text{II}$$

Equation II in the system (D.6) is again the eigenvalue equation for  $A$  and the solution is simply  $|x_{j,2}\rangle = \kappa_i |R_j\rangle$ , where  $\kappa_i$  is a finite complex number. Using this result equation (I) becomes

$$(A - \lambda_j) |x_{j,1}\rangle + (\partial_t A) \kappa_i |R_j\rangle = |R_j\rangle. \quad (\text{D.7})$$

Let  $\{\langle L_j | \}_{j=1, \dots, n}$  denote the set of left eigenvectors of  $A$ , i.e.  $\langle L_j | A = \lambda_j \langle L_j |$  and assume the normalisation  $\langle L_j | R_i \rangle = \delta_{ij}$ . Then  $P := \sum_{i \neq j} \frac{|R_i\rangle \langle L_i|}{\lambda_i - \lambda_j}$  is well defined. Multiplying both sides of equation (D.7) by  $P$  yields

$$\sum_{i \neq j} |R_i\rangle \langle L_i | x_{j,1}\rangle = \sum_{i \neq j} \kappa_i \frac{|R_i\rangle \langle L_i|}{\lambda_i - \lambda_j} (\partial_t A) |R_j\rangle. \quad (\text{D.8})$$

The term  $\sum_{i \neq j} |R_i\rangle \langle L_i|$  on the right hand side of equation (D.8) is a projector to the space  $\mathbb{1} - |R_j\rangle \langle L_j|$  and using equation (B.9) one finds that the right hand side is equal to  $|\partial_t R_j\rangle$ . It follows that the projection of  $|x_{j,1}\rangle$  is equal to  $\kappa_j |\partial_t R_j\rangle$  and therefore

$$|x_{j,1}\rangle = \kappa_j |\partial_t R_j\rangle + \gamma_j |R_j\rangle, \quad (\text{D.9})$$

where  $\gamma_j$  is a complex number. Note that  $|R_j\rangle$  is in the kernel of  $(A - \lambda_j)$ , which means we can add any scalar multiple of  $|R_j\rangle$  to the solution  $|x_{j,1}\rangle$  of equation (I) and get another solution. Exploiting this freedom it is possible to set  $\gamma_j = 0$ . To compute the value of  $\kappa_j$  simply multiply equation (I) by  $\langle L_j|$  from the left. This annihilates the first term on the left hand side and we obtain

$$\kappa_j \langle L_j| (\partial_t A) |R_j\rangle = 1. \quad (\text{D.10})$$

Applying equation (B.6) gives  $\kappa_j = 1/\partial_t \lambda_j$ . Putting everything together yields an analytic expression for the columns of the matrix  $\mathcal{X}$ :

$$|x_{(2j-1)}\rangle = \begin{pmatrix} |R_j\rangle \\ 0 \end{pmatrix} \quad (\text{D.11})$$

$$|x_{2j}\rangle = \frac{1}{\partial_t \lambda_j} \begin{pmatrix} |\partial_t R_j\rangle \\ |R_j\rangle \end{pmatrix}.$$

To compute the columns of  $\mathcal{X}^{-1}$  we start with the equation

$$\mathcal{X}^{-1} \mathcal{B} = \mathcal{J} \mathcal{X}^{-1}, \quad (\text{D.12})$$

which follows directly from equation (D.1). It turns out that it is advantageous to consider the transpose of this equation

$$\mathcal{B}^T \mathcal{Y} = \mathcal{Y} \mathcal{J}^T, \quad (\text{D.13})$$

where  $\mathcal{Y} := (\mathcal{X}^{-1})^T$  is introduced to simplify the notation. The right hand side of equation (D.13) can be written as

$$\begin{pmatrix} y_{1,1} & \cdots & y_{1,2n} \\ \vdots & & \vdots \\ y_{2n,1} & \cdots & y_{2n,2n} \end{pmatrix} \begin{pmatrix} \lambda_1 & 0 & \cdots & \cdots & 0 \\ 1 & \lambda_1 & \ddots & & \vdots \\ 0 & \ddots & \ddots & \ddots & \vdots \\ \vdots & \ddots & \ddots & \lambda_n & 0 \\ 0 & \cdots & 0 & 1 & \lambda_n \end{pmatrix} = \quad (\text{D.14})$$

$$\begin{pmatrix} \lambda_1 y_{1,1} + y_{1,2} & \lambda_1 y_{1,2} & \cdots & \lambda_n y_{1,(2n-1)} + y_{1,2n} & \lambda_n y_{1,2n} \\ \vdots & \vdots & & \vdots & \vdots \\ \lambda_1 y_{2n,1} + y_{2n,2} & \lambda_1 y_{2n,2} & \cdots & \lambda_n y_{2n,(2n-1)} + y_{2n,2n} & \lambda_n y_{2n,2n} \end{pmatrix}$$

The next steps are analogous to the derivation of the columns of  $\mathcal{X}$  above. Let  $|y_i\rangle$  be the  $i$ -th column of  $\mathcal{Y}$ , then (D.14) is equivalent to  $n$  systems of two equations:

$$\mathcal{B}^T |y_{2j}\rangle = \lambda_j |y_{2j}\rangle \quad (\text{D.15})$$

$$\mathcal{B}^T |y_{(2j-1)}\rangle = \lambda_j |y_{(2j-1)}\rangle + |y_{2j}\rangle, \quad (\text{D.16})$$

Equation (D.15) is an eigenvalue equation and the solution is  $|y_{2j}\rangle = \eta_j (0, |R_j^T\rangle)^T$ , where  $|R_j^T\rangle$  is the eigenvector of  $A^T$  to the eigenvalue  $\lambda_j$  and  $\eta_j$  is a scalar constant that will be fixed later by requiring  $\mathcal{Y}^T \mathcal{X} = \mathbb{1}$ .

With the notation  $|y_{(2j-1)}\rangle := (|y_{j,1}\rangle, |y_{j,2}\rangle)^T$  we can rewrite equation (D.16) as a system of two equations:

$$\begin{aligned} (A^T - \lambda_j) |y_{j,1}\rangle &= 0 & \text{I} \\ (\partial_t A^T) |y_{j,1}\rangle + (A^T - \lambda_j) |y_{j,2}\rangle &= \eta_j |R_j^T\rangle & \text{II} \end{aligned} \quad (\text{D.17})$$

Mimicking the steps used to solve the system (D.6) one finds the following expressions for the columns of  $\mathcal{Y}$ :

$$\begin{aligned} |y_{(2j-1)}\rangle &= \frac{\eta_j}{\partial_t \lambda_j} \begin{pmatrix} |R_j^T\rangle \\ |\partial_t R_j^T\rangle \end{pmatrix} \\ |y_{2j}\rangle &= \eta_j \begin{pmatrix} 0 \\ |R_j^T\rangle \end{pmatrix}. \end{aligned} \quad (\text{D.18})$$

The rows of the inverse transformation matrix  $\mathcal{X}^{-1} = \mathcal{Y}^T$  follow immediately from equation (D.18):

$$\mathcal{X}^{-1} = \begin{pmatrix} \frac{\eta_1}{\partial_t \lambda_1} (\langle L_1 |, \langle \partial_t L_1 |) \\ \eta_1 (0, \langle L_1 |) \\ \vdots \\ \frac{\eta_n}{\partial_t \lambda_n} (\langle L_n |, \langle \partial_t L_n |) \\ \eta_n (0, \langle L_n |) \end{pmatrix}, \quad (\text{D.19})$$

where we used the fact that  $|R_j^T\rangle^T = \langle L_j |$ .

To find the values of the complex constants  $\eta_j$  one has to evaluate the product  $\mathcal{X}^{-1} \mathcal{X}$ . In this computation one encounters only four different types of bra-ket products, which are all shown in the following matrix product:

$$\begin{pmatrix} \frac{\eta_i}{\partial_t \lambda_i} (\langle L_i |, \langle \partial_t L_i |) \\ \eta_i (0, \langle L_i |) \end{pmatrix} \begin{pmatrix} |R_j\rangle \\ 0 \end{pmatrix}, \frac{1}{\partial_t \lambda_j} \begin{pmatrix} |\partial_t R_j\rangle \\ |R_j\rangle \end{pmatrix} = \begin{pmatrix} \frac{\eta_i}{\partial_t \lambda_i} \delta_{ij} & 0 \\ 0 & \frac{\eta_i}{\partial_t \lambda_j} \delta_{ij} \end{pmatrix} \quad (\text{D.20})$$

The entry below the diagonal is trivially zero and the super-diagonal entry vanishes because  $\langle L_i | \partial_t R_j\rangle + \langle \partial_t L_i | R_j\rangle = \partial_t (\langle L_i | R_j\rangle) = \partial_t \delta_{ij} = 0$ . With the choice  $\eta_i = \partial_t \lambda_i$  the right hand side of equation (D.20) becomes the unit matrix and the explicit form of the transformation matrices is given by equations (9) and (10) in the main text.

## Appendix E. Efficient deflation of derivatives of the sign function

In this Appendix an efficient algorithm for the deflation of derivatives of the sign function is developed. Let  $|R_i\rangle$  and  $\langle L_i |$  be the left and right eigenvectors of  $A$  to the eigenvalue  $\lambda_i$ , respectively. Considering equation (8) it

is tempting to exploit the sparsity of  $(0, |x\rangle)^T$  to simplify the deflation calculations. However it turns out that it is necessary to define the deflation for general  $|\Phi\rangle := (|x_1\rangle, |x_2\rangle)^T$ . The reason is that the most convenient way to estimate the error of the TSL approximation is via equation (17), i.e. we apply the TSL approximation twice and measure the deviation from unity. Therefore we need a deflation method that works with general input vectors. In analogy to equation (16) we then get

$$\begin{aligned} \text{sgn}(\mathcal{B}) \begin{pmatrix} |x_1\rangle \\ |x_2\rangle \end{pmatrix} &= \underbrace{\sum_{i=1}^k s_i \left\{ \begin{pmatrix} |R_i\rangle \\ 0 \end{pmatrix} [\langle L_i | x_1 \rangle + \langle \partial_t L_i | x_2 \rangle] + \begin{pmatrix} |\partial_t R_i\rangle \\ |R_i\rangle \end{pmatrix} \langle L_i | x_2 \rangle \right\}}_{\text{I}} \\ &\quad + \underbrace{\text{sgn}(\mathcal{B}) \bar{\mathcal{P}}_{2k} \begin{pmatrix} |x_1\rangle \\ |x_2\rangle \end{pmatrix}}_{\text{II}}, \end{aligned} \quad (\text{E.1})$$

where we used the fact that  $\partial_t \text{sgn}(\lambda_i) = 0$  since the sign function is piece-wise constant and introduced the notation  $s_i := \text{sgn}(\lambda_i)$ . Let us now investigate part I of (E.1).

$$\text{I} = \sum_{i=1}^k s_i \left\{ \begin{pmatrix} |R_i\rangle \\ 0 \end{pmatrix} \underbrace{[\langle L_i | x_1 \rangle + \langle \partial_t L_i | x_2 \rangle]}_{c_{1i}} + \begin{pmatrix} |\partial_t R_i\rangle \\ |R_i\rangle \end{pmatrix} \underbrace{\langle L_i | x_2 \rangle}_{c_{2i}} \right\} \quad (\text{E.2})$$

In a practical calculation we are interested in finding an efficient way to compute the coefficients  $c_{1i}$  and  $c_{2i}$ . Note that these coefficients are proportional to the scalar products of  $|\Phi\rangle$  with the odd and even rows of the matrix  $\mathcal{X}^{-1}$  respectively. The same coefficients appear in the projection  $\bar{\mathcal{P}}_{2k} |\Phi\rangle$ , which is needed to compute part II. Apart from  $c_{1i}$  and  $c_{2i}$  the only non-trivial part of the deflation is the computation of  $|\partial_t R_i\rangle$ . As we mentioned earlier, the left and right eigenvectors  $\langle L_i |$  and  $|R_i\rangle$  can be computed with **ARPACK** routines.

The coefficients  $c_{2i}$  are simply scalar products. As we will see later on they appear in several parts of the deflation and therefore it pays off pre-compute and save them.

The first part of the coefficients  $c_{1i}$  is again a scalar product. The computation of the second part is more involved. First we use equation B.10 to get rid of the derivative of the eigenvector:

$$\langle \partial_t L_i | x_1 \rangle = \sum_{j \neq i} \frac{\langle L_i | (\partial_t A) | R_j \rangle \langle L_j | x_2 \rangle}{\lambda_i - \lambda_j} \quad (\text{E.3})$$

Computing all the eigenvectors of  $A$  is in general way too expensive and only the first  $k$  eigenvectors are known explicitly. The trick now is to use the identity

$\sum_{j=k+1}^n \frac{|R_j\rangle \langle L_j | x_2 \rangle}{\lambda_i - \lambda_j} \equiv (\lambda_i - A)^{-1} P_k |x_2\rangle$ , where  $P_k := \sum_{i=k+1}^n |R_i\rangle \langle L_i |$ . Note that the inverse of  $(\lambda_i - A)$  is well defined for  $P_k |x_2\rangle$  and we can write

$$\langle \partial_t L_i | x_1 \rangle = \sum_{\substack{j=1 \\ j \neq i}}^k \frac{\langle L_i | (\partial_t A) | R_j \rangle c_{2j}}{\lambda_i - \lambda_j} + \langle L_i | (\partial_t A) (\lambda_i - A)^{-1} P_k |x_2\rangle \quad (\text{E.4})$$

In practical applications the matrix  $A_{\lambda_i} := (\lambda_i - A)$  is sparse and its inverse can be computed very efficiently with iterative methods. Since the vector  $P_k |x_2\rangle$  in equation (E.4) is the same for all  $\lambda_i$  with  $i \in \{1, \dots, k\}$  it is in principle possible to use a multi-shift inversion algorithm to compute the inversions. In practice, however, we found that the numerical inversion with the (multi-shift) BiCGSTAB algorithm was unstable. To avoid stability issues we used the CG algorithm to find the inverse of the Hermitian matrix  $A_{\lambda_i} A_{\lambda_i}^\dagger$ , from which it is straightforward to compute the inverse of  $A_{\lambda_i}$ .

The vector  $|R_i\rangle$  lies in the kernel of the matrix  $A_{\lambda_i}$ . For this reason and because of numerical errors the vector  $A_{\lambda_i}^{-1} P_k |x_2\rangle$  can have non-zero components in  $|R_i\rangle$  direction. Remember that we normalised the derivative of the eigenvectors such that  $\langle \partial_t L_i | R_i \rangle = 0$ . In order to enforce this normalisation in a numerical calculation we have to project out the spurious  $|R_i\rangle$  component. To this end we define the projection operator  $Q_i$  in the following way

$$Q_i |\psi\rangle := |\psi\rangle - |R_i\rangle \langle L_i | \psi \rangle. \quad (\text{E.5})$$

With this operator we can now write down the final equation for  $\langle \partial_t L_i | x_1 \rangle$  that can be used in numerical calculations

$$\langle \partial_t L_i | x_1 \rangle = \langle L_i | (\partial_t A) \left( \sum_{\substack{j=1 \\ j \neq i}}^k \frac{|R_j\rangle \langle c_{2j}}{\lambda_i - \lambda_j} + Q_i (\lambda_i - A)^{-1} P_k |x_2\rangle \right). \quad (\text{E.6})$$

Analogously one can use equation (B.9) to derive the following formula for the derivative of the right eigenvectors

$$|\partial_t R_i\rangle = \sum_{\substack{j=1 \\ j \neq i}}^k \frac{|R_j\rangle \langle L_j | (\partial_t A) | R_i \rangle}{\lambda_i - \lambda_j} + Q_i (\lambda_i - A)^{-1} P_k (\partial_t A) | R_i \rangle. \quad (\text{E.7})$$

We now have all the parts needed for an efficient computation of the deflation. The whole computation is summarised in the following code listing:

```

1: function DEFLATEDSIGNDERIVATIVE
2:   // Compute  $|out\rangle = (|out_1\rangle, |out_2\rangle)^T = \text{sgn}(\mathcal{B})(|x_1\rangle, |x_2\rangle)^T$ 
3:   // with deflation
4:
5:   for  $i \leftarrow 1$  to  $k$  do // Compute  $|\partial_t R_i\rangle$ 
6:      $|\partial_t R_i\rangle = |0\rangle$ 
7:     for  $j \leftarrow 1$  to  $k$  do
8:       if  $i \neq j$  then
9:          $|\partial_t R_i\rangle = |\partial_t R_i\rangle + \frac{|R_j\rangle \langle L_j | (\partial_t A) | R_i \rangle}{\lambda_i - \lambda_j}$ 
10:      end if
11:    end for
12:     $|\partial_t R_i\rangle = |\partial_t R_i\rangle + Q_i (\lambda_i - A)^{-1} P_k (\partial_t A) | R_i \rangle$ 
13:  end for
14:
15:  for  $i \leftarrow 1$  to  $k$  do // Compute  $c_{2i}$ 
16:     $c2[i] = \langle L_i | x_2 \rangle$ 

```

```

17:   end for
18:
19:   // Compute  $c_{1i}$ , the exact part and the projection of  $|x\rangle$ 
20:    $|x_k\rangle = P_k |x_2\rangle$ 
21:    $|out_1\rangle = |0\rangle$ 
22:    $|out_2\rangle = |0\rangle$ 
23:   for  $i \leftarrow 1$  to  $k$  do
24:      $|v\rangle = Q_i (\lambda_i - A)^{-1} |x_k\rangle$ 
25:     for  $j \leftarrow 1$  to  $k$  do
26:       if  $i \neq j$  then
27:          $|v\rangle = |v\rangle + \frac{c2[j]|R_j\rangle}{\lambda_i - \lambda_j}$ 
28:       end if
29:     end for
30:      $c1[i] = \langle L_i | ((\partial_t A) |v\rangle + |x_1\rangle)$ 
31:     // Exact part of output
32:      $s_i = \text{sgn}(\lambda_i)$ 
33:      $|out_1\rangle = |out_1\rangle + s_i (c1[i] |R_i\rangle + c2[i] |\partial_t R_i\rangle)$ 
34:      $|out_2\rangle = |out_2\rangle + s_i (c2[i] |R_i\rangle)$ 
35:     // Projection of input vector
36:      $|x_1\rangle = |x_1\rangle - (c1[i] |R_i\rangle + c2[i] |\partial_t R_i\rangle)$ 
37:      $|x_2\rangle = |x_2\rangle - (c2[i] |R_i\rangle)$ 
38:   end for
39:   // Exact part plus TSL approximation of projected part
40:    $|out\rangle = (|out_1\rangle, |out_2\rangle)^T + \text{TSL}(\mathcal{B}, (|x_1\rangle, |x_2\rangle)^T)$ 
41:   return  $|out\rangle$ 
42: end function

```

## References

- [1] N. J. Higham, *Functions of Matrices: Theory and Computation*, SIAM, 2008.
- [2] J. Bloch, T. Wettig, Overlap Dirac operator at nonzero chemical potential and random matrix theory, *Phys.Rev.Lett.* 97 (2006) 012003. [arXiv:hep-lat/0604020](#).
- [3] N. Cundy, T. Kennedy, A. Schäfer, A lattice dirac operator for QCD with light dynamical quarks, *Nucl. Phys. B* 845 (2011) 30 – 47. [arXiv:1010.5629](#).
- [4] L. Giusti, C. Hoelbling, M. Lüscher, H. Wittig, Numerical techniques for lattice QCD in the  $\epsilon$ -regime, *Comput.Phys.Commun.* 153 (2003) 31–51. [arXiv:hep-lat/0212012](#).
- [5] J. van den Eshof, A. Frommer, T. Lippert, K. Schilling, H. A. van der Vorst, Numerical Methods for the QCD Overlap Operator: I. Sign-Function and Error Bounds, *Comput.Phys.Commun.* 146 (2002) 203–224. [arXiv:hep-lat/0202025](#).
- [6] A. D. Kennedy, Approximation Theory for Matrices, *Nucl.Phys.Proc.Suppl.* 128C (2004) 107–116. [arXiv:hep-lat/0402037](#).
- [7] J. C. R. Bloch, T. Brey, A. Frommer, S. Heybrock, K. Schäfer, T. Wettig, Short-recurrence Krylov subspace methods for the overlap Dirac operator at nonzero chemical potential, *Comput.Phys.Commun.* 181 (2010) 1378–1387. [arXiv:0910.1048](#).
- [8] J. Bloch, T. Brey, T. Wettig, Comparing iterative methods to compute the overlap Dirac operator at nonzero chemical potential, *PoS LATTICE 2008:027*. [arXiv:0810.4228](#).
- [9] J. Bloch, S. Heybrock, A nested Krylov subspace method to compute the sign function of large complex matrices, *Comput.Phys.Commun.* 182 (2011) 878–889. [arXiv:0912.4457](#).
- [10] M. Pühr, P. V. Buividovich, A method to calculate conserved currents and fermionic force for the lanczos approximation to the overlap dirac operator, *PoS LAT2014* (2014) 047. [arXiv:1411.0477](#).
- [11] G. H. Golub, C. F. Van Loan, *Matrix Computations*, 3rd Edition, The Johns Hopkins University Press Baltimore and London, 1996.
- [12] R. Mathias, A chain rule for matrix functions and applications, *SIAM J. Matrix Anal. & Appl.* 17 (1996) 610 – 620.
- [13] R. B. Lehoucq, D. C. Sorensen, C. Yang, *ARPACK Users' Guide: Solution of Large-Scale Eigenvalue Problems with Implicitly Restarted Arnoldi Methods*, SIAM, 1998.
- [14] N. Cundy, S. Krieg, G. Arnold, A. Frommer, T. Lippert, K. Schilling, Numerical Methods for the QCD Overlap Operator IV: Hybrid Monte Carlo, *Comput.Phys.Commun.* 180 (2009) 26–54. [arXiv:hep-lat/0502007](#).

- [15] Z. Fodor, S. D. Katz, K. K. Szabo, Dynamical overlap fermions, results with hybrid Monte-Carlo algorithm, JHEP 0408 (2004) 003. [arXiv:hep-lat/0311010](#).
- [16] M. Lüscher, P. Weisz, On-shell improved lattice gauge theories, Comm. Math. Phys. 97 (1-2) (1985) 59–77.
- [17] C. Gattringer, R. Hoffmann, S. Schaefer, Setting the scale for the Lüscher-Weisz action, Phys.Rev.D 65 (2002) 094503. [arXiv:hep-lat/0112024](#).
- [18] Z. Xianyi, et al., OpenBLAS. <http://www.openblas.net>
- [19] C. Gattringer, P. E. L. Rakow, A. Schaefer, W. Soeldner, Chiral symmetry restoration and the  $Z_3$  sectors of QCD, Phys.Rev.D 66 (2002) 054502. [arXiv:hep-lat/0202009](#).
- [20] S. J. Dong, K. F. Liu, Stochastic Estimation with  $Z_2$  Noise, Phys.Lett. B 328 (1994) 130–136. [arXiv:hep-lat/9308015](#).
- [21] R. Mathias, A Chain Rule for Matrix Functions and Applications, SIAM J. Matrix Anal. & Appl. 17 (3) (1996) 610–620.
- [22] K. Fukushima, D. E. Kharzeev, H. J. Warringa, The Chiral Magnetic Effect, Phys.Rev.D 78 (2008) 074033. [arXiv:0808.3382](#).
- [23] G. M. Newman, D. T. Son, Response of strongly-interacting matter to magnetic field: some exact results, Phys.Rev.D 73 (2006) 045006. [arXiv:hep-ph/0510049](#).
- [24] M. A. Metlitski, A. R. Zhitnitsky, Anomalous axion interactions and topological currents in dense matter, Phys.Rev.D 72 (2005) 045011. [arXiv:hep-ph/0505072](#).